Available online at www.sciencedirect.com
SCIENCE DIRECT®
Mathematical Biosciences 200 (2006) 152–169
Mathematical Biosciences
www.elsevier.com/locate/mbs

The SIRC model and influenza A

Renato Casagrandi [a,*], Luca Bolzoni [b], Simon A. Levin [c], Viggo Andreasen [d]

[a] *Dipartimento di Elettronica e Informazione, Politecnico di Milano, Via Ponzio 34/5, 20133 Milano, Italy*
[b] *Dipartimento di Scienze Ambientali, Università degli Studi di Parma, 43100 Parma, Italy*
[c] *Department of Ecology and Evolutionary Biology, Princeton University, Princeton, NJ 08544, USA*
[d] *Department of Mathematics and Physics, Roskilde University, DK-4000 Roskilde, Denmark*

Received 31 January 2005; received in revised form 6 October 2005; accepted 22 December 2005
Available online 28 February 2006

Abstract

We develop a simple ordinary differential equation model to study the epidemiological consequences of the drift mechanism for influenza A viruses. Improving over the classical SIR approach, we introduce a fourth class (C) for the cross-immune individuals in the population, i.e., those that recovered after being infected by different strains of the same viral subtype in the past years. The SIRC model predicts that the prevalence of a virus is maximum for an intermediate value of R_0, the basic reproduction number. Via a bifurcation analysis of the model, we discuss the effect of seasonality on the epidemiological regimes. For realistic parameter values, the model exhibits a rich variety of behaviors, including chaos and multi-stable periodic outbreaks. Comparison with empirical evidence shows that the simulated regimes are qualitatively and quantitatively consistent with reality, both for tropical and temperate countries. We find that the basins of attraction of coexisting cycles can be fractal sets, thus predictability can in some cases become problematic even theoretically. In accordance with previous studies, we find that increasing cross-immunity tends to complicate the dynamics of the system.
© 2006 Elsevier Inc. All rights reserved.

Keywords: SIR and SIRS models; Epidemics; Cross-immunity and boosting; Bifurcation analysis; Multi-stability and fractal basins; Chaos

* Corresponding author. Tel.: +39 02 2399 3471; fax: +39 02 2399 3412.
E-mail addresses: casagran@elet.polimi.it (R. Casagrandi), luca.bolzoni@nemo.unipr.it (L. Bolzoni), slevin@eno.Princeton.EDU (S.A. Levin), viggo@ruc.dk (V. Andreasen).

0025-5564/$ - see front matter © 2006 Elsevier Inc. All rights reserved.
doi:10.1016/j.mbs.2005.12.029

1. Introduction

In the common wisdom, influenza is perceived as an ephemeral and feeble fever, like a little tax to be paid for by most of us every few 'flu seasons'. Unfortunately, this picture is untrue. In reality, influenza is an important problem for the public health system. Just to give an idea of the social costs due to morbidity, we point out that the excess hospitalizations for pneumonia and influenza during the most recent epidemics in the United States have been estimated to have cost up to US$10 billion [1]. This amount should be increased by the costs of workdays lost by the people infected, vaccines, antiviral drugs and so on. Extremely difficult to evaluate [2], yet most important, there is an excess of mortality associated with complications due to influenza, especially in the elderly [3]: the flu epidemics during the two decades 1972–1992, for example, induced an average of 21 000 deaths per season in the US [4].

Influenza is caused by a virus that can be of three different types (A, B and C, see [5]). Among these types, the virus A is epidemiologically the most important for humans, since it can recombine its genes with those of strains circulating in animal populations (birds, swine and horses). These relatively rare recombinations give rise every few decades to new viral subtypes via the so called *antigenic shift* mechanism [6]. The new subtypes, classified according to the antigenic and genetic nature of their surface glycoproteins HA (hemagglutinin) and NA (neuraminidase), are usually antigenically so different from their ancestors to escape completely the defenses of the immune system of the previously infected hosts. Consequently, every antigenic shift is associated potentially with particularly severe pandemics: the Spanish flu in 1918 or the Hong Kong influenza in 1968, caused by the genesis of the H1N1 and H3N2 subtypes respectively, are but two major examples (see [2] for others). Like B, the influenza A virus is also subject to point mutations in the HA and NA genes that induce an *antigenic drift* of the viral strains in each subtype. These minor mutations, which occur at a faster time scale with respect to shifts, are the underlying causes of the influenza epidemics that we experience every year [5,7]. Much evidence [8–10] shows that the antigenic distance between two different strains influences the degree of partial immunity, often called *cross-immunity*, conferred to a host already infected by one of the strains with respect to the other.

Many mathematical models have been proposed in the literature to describe the inter-pandemic ecology of influenza A in humans (see [11] for a review). A typical approach is that of modelling the interactions between individuals that are (or have been) infected by different viral strains. To this end, multiple SIR (susceptibles-infectives-recovered) models can be connected via some cross-immunity parameters [12,13]. The analysis of these models has shown that multiple strains of influenza can persist in the human populations and that their prevalence can exhibit self-sustained oscillations through time. In a recent extension to these pioneering studies, Lin et al. [14] estimated the drift speed of the travelling wave solutions arising in a model where the virus mutation is described as a diffusion process in a linear, continuous strain space. Stochastic, individual based models aimed to understanding the dynamics of evolving diseases over discrete strain spaces and for finite populations are proposed in [15]. The major drawback of the multi-strain models is that their analysis can become analytically difficult or numerically cumbersome if the number of strains is large enough to mimic the real variety in nature (but see [16]). An alternative path to viewing the emergence of new viral strains is that of introducing into the model a loss of immunity by the host, as originally suggested by Pease [17] for the case of influenza A. Pease based his evolutionary

model on some data by Gill and Murphy [18] and Potter et al. [19], who experimentally showed that the probability of recovered individuals being reinfected by new circulating strains linearly increases with the time since last infection. Both the genetic and the antigenic evolution of influenza A viruses occurs indeed linearly through time, as emphasized in a detailed study by Smith et al. [20] and discussed below. These results indicate that the classical single-strain SIRS model [21] cannot be used *as is* to study influenza. Gomes and colleagues [22] recently proposed to consider a 'temporary partial immunity' for the individuals in the R compartment to solve the issue. Here we introduce a new compartment C, which can be called *cross-immune*, to design an intermediate state between the fully susceptible state (S) and the fully protected one (R). Only by extending the SIR model with a new class one can indeed account for the fact that, when the cross-immune hosts are exposed to antigenically similar – but different – strains, their pre-existing immune responses are boosted [23,24], as in the case of pertussis [25,26]. Epidemic models of temporary partial immunity – or variable susceptibility – were first introduced by Kermack and McKendrick [27] and have recently been studied in the context of influenza [28,29].

The article is organized as follows. First we introduce the SIRC model, which is a fourth-order ODE system, and we analyze its behavior. Without accounting for seasonality, its dynamics is extremely simple, yet different from that of the classical SIR-like models. Our bifurcation analysis of the seasonally forced SIRC model shows that it can predict a rich variety of complex temporal patterns that are realistic for influenza A. Then, we compare some simulations obtained with the SIRC model against empirical data, from both the tropical and the temperate regions, and show that the predicted behaviors are qualitatively and quantitatively in accordance with observations. We also show that some basins of attraction of the periodic regimes in the model really have fractal nature. Comments on the role played by cross-immunity and boosting in shaping the complexity of the epidemiological regimes close the paper.

2. The SIRC model

The general flow diagram of the SIRC model is shown in Fig. 1. From an epidemiological viewpoint, a human community can be subdivided at any time t into four compartments with respect to the dominant circulating strain of an influenza A subtype: the proportion of susceptibles $S(t)$, i.e., those who do not have specific immune defenses against that particular strain; the fraction $I(t)$ of those individuals that are infected by the current dominant strain, thus infective; the two classes of those who are totally or partially immune to that strain (i.e., recovered $R(t)$ and cross-immune $C(t)$, respectively). At a first glance, disregarding the epidemiology of the subdominant viral

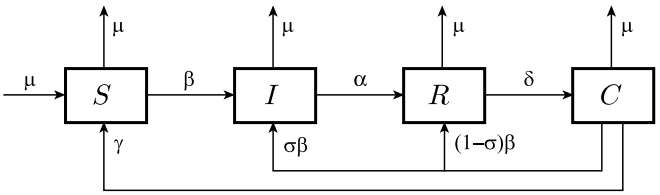

Fig. 1. General flow diagram of the SIRC model (1).

strains could seem too crude a hypothesis, but there is both empirical [30–32] and theoretical [33] evidence that the dominant strain plays a very major role during epidemics. As in other status-based approaches, we assume a highly symmetric topology of viral strain space with constant cross-immunity irrespective to the number of reinfections (see [34] for a more sophisticated multi-strain approach).

The novelty of the flow diagram in Fig. 1 with respect to those of other SIRS-like models – see for example Fig. 3 in Anderson and May [35, p. 364], or Fig. 1(b) in Pease [17, p. 424] – is that, after recovery from an infection, the individuals enter a new class, C. More precisely, the individuals in the R class are those who have recovered from the dominant strain currently circulating and against which they have full immunity. Then, after some period of time, the individuals move to the C class because they have only partial immunity to a new dominant strain that has emerged since they were last infected. Thus, the movements of individuals among different immune classes are caused by the fact that we use a moving frame in immune space, exactly as in Pease's approach [17]. While in the C compartment, the individuals are exposed to the currently dominant strain at the same contact rate (β) of the susceptibles (S). However, only a fraction σ of the exposed cross-immune individuals are recruited in a unit time into the infectives compartment I. We assume a positive immune response for the remaining fraction of exposed individuals, who are then recruited into the R compartment (complete boosting).

Formally, the SIRC model can be represented by the following set of four ordinary differential equations

$$\dot{S} = \mu(1 - S) - \beta SI + \gamma C, \tag{1a}$$

$$\dot{I} = \beta SI + \sigma\beta CI - (\mu + \alpha)I, \tag{1b}$$

$$\dot{R} = (1 - \sigma)\beta CI + \alpha I - (\mu + \delta)R, \tag{1c}$$

$$\dot{C} = \delta R - \beta CI - (\mu + \gamma)C, \tag{1d}$$

where each of the six parameters μ, α, β, γ, δ and σ has a clear epidemiological meaning, as we discuss in the next paragraph, thus can be estimated from data. It is important to remark that Eq. (1b) does not account for the virulence of the dominant strain, usually defined in SIR-like models as the extra mortality induced by the pathogen to the infected hosts. This is because we assume that morbidity is more important than mortality for influenza.

2.1. Estimating the parameter values

The parameter μ represents the mortality rate in every compartment and is assumed to equal the rate of newborns in the population (because population size is assumed to be constant), who are supposed to be susceptible individuals. Its inverse (μ^{-1}) can be easily calibrated as the average lifetime of human hosts.

The parameters α, δ and γ are the inverses of the average time spent by the individuals in each of the three compartments I, R and C respectively. While the value of the infectious period (α^{-1}) can be estimated on the basis of clinical observations only – such a value varies between 2 and 7 days for flu [36,37] – assigning numerical values to the totally immune (δ^{-1}) and the cross-immune period (γ^{-1}) is more difficult and requires further information.

From genetic studies on influenza A subtypes drift, we know that the phylogenic trees of H3N2 and H1N1 are cactus-like [38], in the sense that many short-living side lineages depart from a main trunk of the evolutionary tree, where the successful lineage is displayed. More precisely, season-by-season analyses of viral evolution show that, while the genetic distance between isolated strains increases linearly with time, the antigenic distance between them is more punctuated, growing linearly but in a stepwise way (see Fig. 4 in [20]). In general, single amino acid substitutions are indeed not sufficient to escape the hosts' immunological defenses and more changes must accumulate. In other words, from an antigenic viewpoint different isolated strains can be grouped into clusters [39,20]. Since the temporally adjacent dominant clusters overlap, we assume that the individuals lose their complete immunity every time a new dominant cluster invades the viral arena. The parameter δ can thus be estimated as the average time of appearance of new dominant clusters. Studies on Weekly Epidemiological Records (see Fig. 3 in [39]) revealed that 9 dominant antigenic clusters emerged during 16 seasons (1984–2000), indicating an average period of approximately 1.77 years. On a longer time horizon, since the WHO changed 20 viral prototypes for composing the vaccines during the period 1973–2001, Hay et al. [40] estimated that new dominant antigenic variants of H3N2 emerge every 1–2 years.

The average antigenic (Hamming) distance between two subsequent clusters is around 4.5 units [20] and it is believed that there is cross-reactivity among strains only if their antigenic distance is between 0 and 7 units [41]. Therefore, we can assume that the average residence time of individuals in class C closely relates to the average lifetime of a single cluster, i.e., the one emerging just after the dominant cluster of the strain those individuals have been infected by. Available data show that the average lifetime of dominant clusters varies between 2 and 5 years [42,39].

The parameter σ can be viewed as the average reinfection probability of a cross-immune individual. Thanks to Pease [17], we know that the reinfection probability linearly increases with the time since last infection at a rate r of approximately 0.026 years^{-1}. A plausible value for σ can thus be

$$\sigma \cong r[\delta^{-1} + \gamma^{-1}], \tag{2}$$

where the terms in the parentheses simply stay for the mean time passed since last infection for a cross-immune individual. In fact, as remarked above, δ^{-1} and γ^{-1} represent the time averagely spent by an individual in classes R and C, respectively. Thus, considering the departure from class I of all the cross-immune individuals as their birth, the terms in parentheses of Eq. (2) are nothing but the average of their ages. From a mathematical viewpoint, it is interesting to notice that, in the

Table 1
Minimum (min) and maximum (max) values to be attributed to the parameters of model (1) to study influenza A

Parameter	Min	Max	References
μ	1/80 y^{-1}	1/40 y^{-1}	–
α	365/7 y^{-1}	365/2 y^{-1}	[36,37]
γ	1/5 y^{-1}	1/2 y^{-1}	[42,39,20]
δ	1/2 y^{-1}	1 y^{-1}	[40,39]
σ	0.05	0.2	[19,17]
R_0	2	10	[50,88,16,14,89,33,90]

The symbol y stays for years.

absence of cross-immunity ($1-\sigma=0$), the two classes S and C are immunologically indistinguishable, since

$$\dot{S}+\dot{C}=\mu[1-(S+C)]-\beta(S+C)I+\delta R.$$

Consequently, in the limit of $\sigma\to 1$, the SIRC model reduces to the classical SIRS.

In Table 1, we summarize the ranges of variation for the values to be attributed to the parameters for studying influenza A. The value to be attributed to parameter β can be problematic and is discussed extensively in the next section.

3. Model behavior

It can be easily shown that the non-linear SIRC model (1) is a positive system [43]. This means that its state variables remain non-negative for any trajectory initialized at non-negative conditions. By substituting $I=0$, i.e., a value that nullifies the right-hand side of Eq. (1b), into the other conditions for system stationarity ($\dot{S}=\dot{R}=\dot{C}=0$), we find that the vector $\overline{X}_0=[\,\overline{S}_0\quad\overline{I}_0\quad\overline{R}_0\quad\overline{C}_0\,]^{\mathrm{T}}=[\,1\quad 0\quad 0\quad 0\,]^{\mathrm{T}}$ is always an equilibrium of the SIRC model. The Jacobian matrix associated with the *disease-free equilibrium* $\overline{X}_0$ is an upper triangular matrix whose diagonal elements are $\{-\mu,-(\mu+\gamma),-(\mu+\delta),\beta-(\mu+\alpha)\}$. Thus $\overline{X}_0$ is an asymptotically stable node if and only if

$$R_0=\frac{\beta}{\mu+\alpha}<1.$$

The quantity R_0 is the basic reproduction number [44,35], i.e., the average number of secondary infections caused by a single primary infection in a totally susceptible population. For $R_0>1$, the disease-free equilibrium is instead a saddle and, in this case, there exists a unique positive *endemic equilibrium*, called $\overline{X}_+=[\,\overline{S}_+\quad\overline{I}_+\quad\overline{R}_+\quad\overline{C}_+\,]^{\mathrm{T}}$. Its uniqueness can be proved by solving the algebraic system obtained when imposing the time derivatives (1) equal zero. After some simple manipulations, one is left with the solution of a second-order equation of the kind $a\overline{I}_+^2+b\overline{I}_++c=0$, where a is positive independently of the parameter values, c is negative if and only if $R_0>1$, and b can possibly be negative only when c is negative. Given these constraints, the positivity and uniqueness of $\overline{X}_+$ are guaranteed if and only if $R_0>1$. Moreover, the linearized system around the endemic equilibrium is asymptotically stable, as can be proved by Hurwitz's criterion. Thus $\overline{X}_+$, whenever it exists, is always asymptotically stable in the SIRC model. In conclusion, one can summarize the analysis by saying that a transcritical bifurcation of equilibria occurs in the system when R_0 crosses unity. If loss of immunity depends on the time since last infection, then the endemic equilibrium can be unstabilized through a Hopf-bifurcation [29].

Despite the strong similarities between the nature of the equilibria in a traditional SIRS (see for example [45]) and the SIRC model, the two systems do not behave identically. Fig. 2 shows the prevalence of the disease at the endemic equilibrium ($\overline{I}_+$) as a function of the contact rate (β) both for the SIRC (solid) and a SIRS model (dashed). While in the SIR/SIRS models the prevalence monotonically increases with β [46], in our model there is a finite value of the contact rate (β^*) that maximizes it. This qualitative difference can be intuitively understood as follows. Large values of β imply a high probability that a cross-immune individual enters in contact with a different dominant

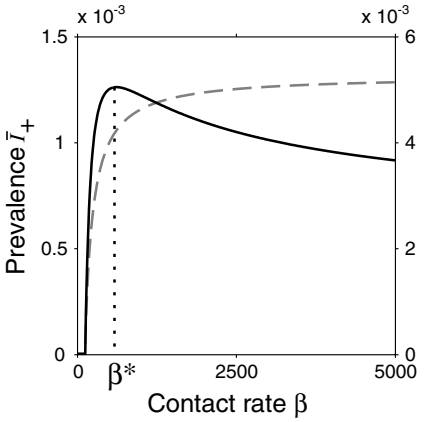

Fig. 2. Prevalence of the virus at the equilibrium ($\bar{I}_+$) as a function of the contact rate (β) either in a SIRC (solid curve, left axis) and a SIRS model (dashed, right axis). The parameter values for both models have been fixed to $\mu = 0.02$, $\alpha = 365/3$, $\delta = 1.6^{-1}$, and (SIRC only) $\sigma = 0.07874$, $\gamma = 0.35$.

strain of the same subtype of influenza she/he has already been infected by. Because the immune defenses of such an individual can eventually be boosted, she/he can be bounced back to the R class, thus being fully protected for a longer time from further infections. At the population scale, the global result is a delay into the spread of the disease and lower prevalence. Note that cross-immunity and booster effects are the only constraints here to the maximization of transmissibility. Virulence, which is considered the typical epidemiological quantity limiting the increase of R_0 (see [47–49]), is not even present in Eq. (1b). As a curiosity, it is also worth noticing that the value of β^* obtained in Fig. 2 by setting all other parameters within ranges that are realistic for influenza A (see Table 1) gives an $R_0 = R_0^*$ approximately close to 5, also a plausible value for the disease [50,16,14].

Another important epidemiological quantity is maximized at $\beta = \beta^*$, the disease annual incidence. It can be defined as

$$J = \frac{1}{T}\int_0^T \beta[S(\xi) + \sigma C(\xi)]I(\xi)\,\mathrm{d}\xi, \quad T = 1 \text{ year}$$

and, since $\dot{I} = 0$ at the equilibrium, the function under the integral sign above is constant over time and proportional to prevalence (see again Eq. (1b)). Thus, $J = (\mu + \alpha)\bar{I}_+$.

Also, by choosing other parameter values as in Fig. 2, the time to reinfection for the SIRC model at the equilibrium when $\beta = \beta^*$, which can be evaluated as

$$T_{\text{reinf}} = \frac{\gamma}{\beta\bar{I}_+ + \gamma}\left(\frac{1}{\delta} + \frac{1}{\gamma} + \frac{1}{\beta\bar{I}_+}\right) + \frac{\beta\bar{I}_+}{\beta\bar{I}_+ + \gamma}\left[\sigma\left(\frac{1}{\delta} + \frac{1}{\beta\bar{I}_+}\right) + (1-\sigma)T_{\text{reinf}}\right]$$

is approximately 5.37 years, in accordance with experimental evidence for both influenza A [24] and B [51].

3.1. The effects of seasonality

As we know from everyday experience, seasonality is such a crucial component of influenza [11] that 'flu season' and 'winter season' are practically synonymous at mid-latitudes. The three most

typical explanations of seasonality in this context are pathogen appearance and disappearance via regular annual migration [52], variations in host susceptibility caused by physiological processes [53] and environmental changes [54]. Mysteriously, however, empirical studies clarifying the exact role played by each of the advocated underlying causes of seasonality are still scarce.

As traditionally done for the study of childhood diseases since the early 70s [55,56], we can introduce seasonality into the SIRC model by assuming that virus transmissibility varies periodically through time, with a yearly cycle. To this end, we can model the contact rate in the simplest form as a sinusoidal function of t [57], i.e.,

$$\beta(t) = \beta_0(1 + \varepsilon\cos(2\pi t)), \tag{3}$$

where the two parameters β_0 and $0 \leqslant \varepsilon \leqslant 1$ represent the baseline rate of transmission and the degree of seasonality, respectively. By substituting Eq. (3) into model (1) we obtain a periodically forced non-linear system whose behavior is too complex to be investigated analytically. Since empirical estimates of β are hard to be found in general [46] and particularly for influenza (see the caveat in [58]), it is important to understand how the behavior of the SIRC model changes under wide variations of the values attributed to the parameters ε and β_0 that fully describe the contact rate. Technically, bifurcation analysis [59] is the most appropriate tool in these cases and it can be performed numerically via specialized software implementing continuation techniques, such as LOCBIF [60] or AUTO [61].

Our bifurcation analysis of the seasonally forced SIRC model in the parameter space (ε, β_0) is shown in Fig. 3. Unsurprisingly, provided that the endemic equilibrium exists in the unforced model, i.e., above the dotted line $\beta_0 = \mu + \alpha$ of Fig. 3, a very small degree of seasonality is sufficient to induce a long-term periodic behavior in the system. The only attractor in region 0 of

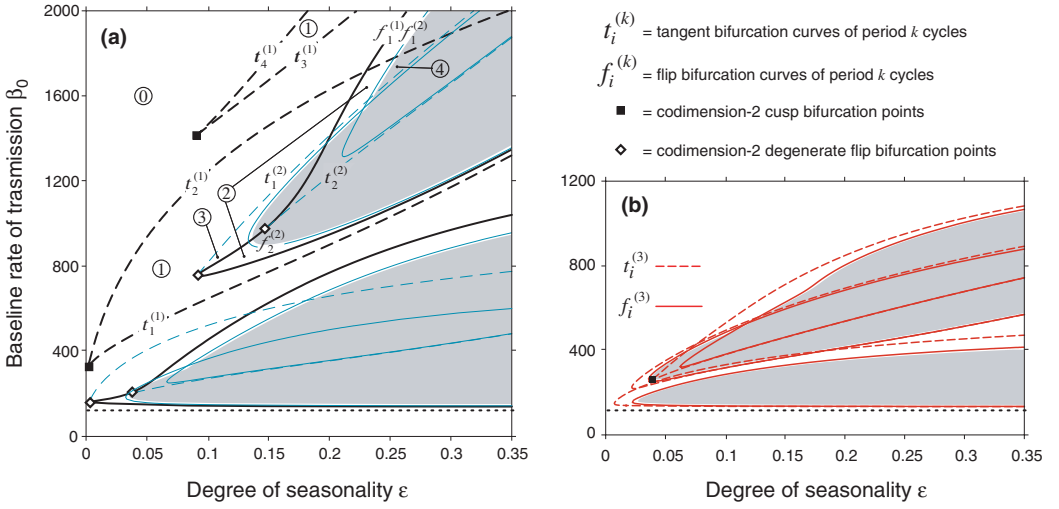

Fig. 3. Bifurcation curves of the seasonally forced SIRC model (1) involving (a) period-one and period-two attractors (in black and blue, respectively), and (b) period-three attractors (in red). The model behavior is chaotic for parameter settings within the gray regions (see text for details). Other parameter values as in Fig. 2. (For interpretation of color in this figure, the reader is referred to the web version of this article.)

Fig. 3(a) is indeed a period-one cycle. The black squares in the same panel are codimension-2 cusp bifurcation points and the two curves $t_i^{(1)}$ departing from each of them are tangent bifurcations of cycles: in regions 1, thus, a pair of period-one cycles (one stable and the other unstable) coexist with the original stable period-one solution of region 0. The curve $f_1^{(1)}$ is a flip bifurcation one: by crossing it and entering regions 2, the original period-one cycle loses its stability in favor of a period-two stable solution. This period-two cycle also undergoes a supercritical flip bifurcation $[f_1^{(2)}]$ for greater degrees of seasonality, that is, it becomes unstable, giving rise to a period-four stable cycle. A sequence of period-doubling bifurcations $f_1^{(4)}, f_1^{(8)}, \ldots, f_1^{(\infty)}$ accumulates then so closely to $f_1^{(2)}$ that we have been unable to continue the curves numerically after detection. Beyond $f_1^{(\infty)}$, the SIRC model behaves chaotically and this is why we have painted in gray the area within the curve $f_1^{(2)}$. The white diamonds on the flip curve $f_1^{(1)}$ mark two codimension-2 degenerate flip bifurcation points: in the segment of $f_1^{(1)}$ delimited by the two diamonds the flip bifurcation is subcritical and, at each of the degenerate points, a tangent bifurcation curve of period-two cycles originates (see [62] for details). In terms of attractors, region 3 is thus characterized by two period-one cycles (see region 1 above) and one period-two cycle. For greater ε's, the period-two attractor undergoes a supercritical flip bifurcation and the flip curve $f_2^{(2)}$ is simply the first of a second cascade of period-doubling bifurcations bringing the SIRC model to behave chaotically in the gray region.

The bifurcation scheme of the seasonally forced model (1) in the lower zone of the (ε, β_0)-plane is more complex than the one just described above. In terms of bifurcations involving period-one and period-two periodic attractors, apart from the tangent bifurcations arising from cusp points, a one-to-one correspondence can be made between the curves we have continued in the upper portion of the parameter space and those in its lower portion, as the reader can inspect simply by visual comparison (see again Fig. 3(a)). In particular, the presence of complete cascades of period-doubling bifurcations ensure that there is another region in the (ε, β_0)-plane, also painted in gray, where the SIRC model has chaotic dynamics. The greater complexity of the parametric portrait of the SIRC model for low β_0's is caused by the bifurcation curves involving period-three attractors, as shown in Fig. 3(b). A pair of period-three periodic solutions (one stable and the other unstable) originate, indeed, while entering the convex region formed by each of the dashed curves $t_i^{(3)}$. The stable period-three cycles then lose their stability through the supercritical flip bifurcation curves $f_i^{(3)}$, and aperiodic regimes are suddenly reached via Feigenbaum cascades.

By merging the two panels of Fig. 3 and restricting our attention to the range of transmissibility values appropriate for the viral strains of influenza A, i.e., such that $2 \leqslant R_0 \leqslant 10$, we obtain the parametric portrait of Fig. 4. Colored regions in that figure indicate parametric conditions where either multiple periodic outbreaks can coexist or the behavior is chaotic. The attractors for parameter values in the blue [magenta] regions have been originated by period-one or two [three] cycles. The darker the shade, the more complex is the behavior of the SIRC model. Since the uncolored portion of parameter space (ε, β_0) is very limited, it is clear that the SIRC model predicts a rich variety of behaviors for influenza other than the simple annual recurrence.

Albeit the traditional SIR model can also exhibit chaos if seasonally forced [63], its bifurcation diagram is substantially simpler than the one obtained for the SIRC model (see [64] for a direct comparison). The question on how the predicted regimes contrast to epidemiological time series for influenza is discussed in the following section.

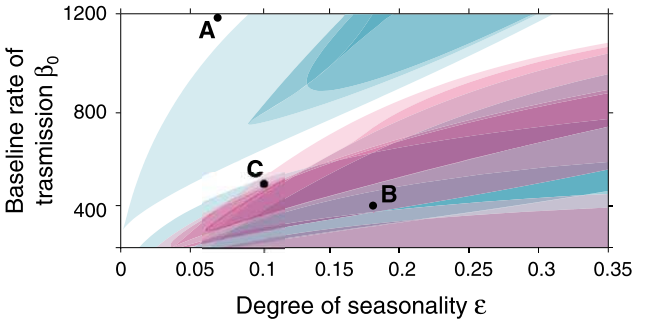

Fig. 4. Parametric portrait of the seasonally forced SIRC model (1) obtained by merging the two panels of Fig. 3. (For interpretation of color in this figure, the reader is referred to the web version of this article.)

4. Epidemiological time series and model predictions

Building time series of subtyped influenza isolates is not an easy task, because it requires laboratory analyses. More frequently, flu time series are built from 'influenza-like illness' cases (ILI). In fact, data are usually collected via clinicians who are asked to judge if an influenza virus is the basis for the patient's symptoms by simply considering a combination of epidemiological and clinical factors, but without requiring laboratory confirmation. Since the prevalence $I(t)$ of the disease in our model is defined as the fraction of individuals carrying the current dominant strain of an influenza subtype, we must deal with subtyped data in order to contrast the model predictions with real dynamics. Many empirical sources provide evidence that flu epidemics have different characteristics around the globe. In our minimal framework, we follow Simonsen [65, see her Fig. 1] by distinguishing data into two major categories only: tropical and temperate epidemiological regimes.

4.1. Tropical regimes

A biannual epidemic cycle caused by the dominant strain with two peaks of activity is a very general pattern for influenza in the tropics (see data in [66] and references in [67]). The exact timing of the two peaks and the difference in their amplitudes can vary from place to place. In Thailand, for example, the outbreaks can occur during spring and autumn months [65], while in Singapore [68,66] they occur in the summer and winter seasons. Another important characteristic of the tropical regime is the considerable background activity in between the two peaks [69]. In terms of parameter values, densely inhabited areas in the tropics – like Bangkok, Hong Kong or Singapore – can be described by low degrees of seasonality (because of the latitude) and high baseline rates of transmission (because of the social context). Indeed, since the host population density N of our model is constant and set to unity, it is realistic to assume that $\beta_0 = \beta_0(N)$ and logical to imagine that $\mathrm{d}\beta_0(N)/\mathrm{d}N$ be positive. Highly urbanized, small countries in the tropics – such as Hong Kong or Singapore – reach population densities that are one order of magnitude higher than densities of any other country at temperate latitudes. Since the transmission rate is influenced by many underlying causes, it is practically impossible to find the exact values for β_0

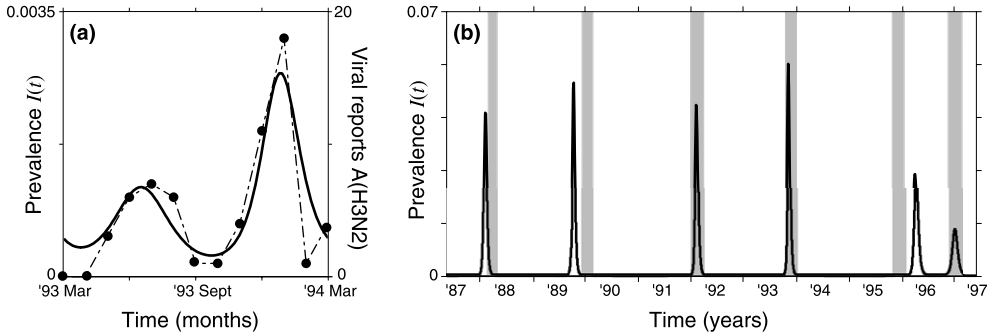

Fig. 5. The prevalence of the dominant strain $I(t)$ obtained with the SIRC model (solid curve, left axis) is contrasted to data. The contact rate in the model is assumed to be maximum at the spring equinox for (a) and in December for (b). Parameter values as in point A of Fig. 4 ($\varepsilon = 0.07$, $\beta_0 = 1200$) for (a) and as in point B ($\varepsilon = 0.18$, $\beta_0 = 400$) for (b). As for the data, the dashed and dotted line in (a, right axis) connects the viral isolates of influenza A of subtype H3N2 in Singapore from March 93 to March 1994 (data from [68]). The gray strips in (b) indicate the weeks when viral strains of influenza A (subtype H3N2) have been isolated in England and Wales (data from [74]).

and ε that describe any particular situation. However, it is still possible to qualitatively compare the model generated regimes with laboratory confirmed data. To this end, we simulate the SIRC model for arbitrarily selected parameter values that are in the biologically plausible range for the tropical regions (i.e., in the top-left part of Fig. 4), like for example point A. In Fig. 5(a) such a simulation is contrasted to the viral isolates of influenza A (subtype H3N2) in Singapore during the period March 1993–March 1994 (data from [68]): the two regimes are indeed very similar. Chew et al. [68] have also analyzed the temporal correlation between the outbreaks of influenza A(H3N2) shown in Fig. 5(a) and the extreme values of some potential environmental drivers of the transmission rate, such as temperature and rainfall. For all the drivers, their study resulted in approximately null correlation coefficients: an outcome that is in line with the SIRC model prediction. In fact, the prevalence time series $I(t)$ of Fig. 5(a) peaks when the transmission rate $\beta(t) \cong \beta_0$, meaning that the forcing wave and the model output are in phase opposition. Also, according to the simulated time series, the annual incidence

$$J = \frac{1}{T}\int_0^T \beta(\xi)[S(\xi) + \sigma C(\xi)]I(\xi)\,\mathrm{d}\xi, \quad T = 1 \text{ year} \tag{4}$$

i.e., the average fraction of the population that has been infected by the virus during 1 year, amounts to 13%, a value that is quantitatively in good accordance with empirical evidence for tropical countries (see, for example, [70,71]).

4.2. Temperate regimes

In temperate regions, influenza occurs every year, in the sense that the ILI time series usually peaks once per year in winter (see [72]). However, the underlying subtyped data show a much less regular pattern. Epidemics of each influenza A subtype, in fact, occur aperiodically as clearly evidenced by data from the US [73], the Netherlands [74] and the UK [11]. The average return time, also called peak-to-peak return time [75], of subtyped epidemics varies between 1 and 3 years for

various subtypes of influenza A [76]. The H3N2 data published by [74], for example, reveal an average return period of about 1.7 years both in The Netherlands and in England and Wales. A return time of about 2 years is also typical for the B virus [5,51].

Compared to tropical countries, temperate regions are characterized by higher degrees of seasonality (ε) and lower baseline rates of transmission (β_0). In order to qualitatively reproduce via simulation the epidemiological regime of an influenza viral subtype in a temperate country, we can select a point in the biologically plausible range of parameter values for the temperate regions, i.e., the central-bottom zone of the (ε, β_0) space in Fig. 4. That parametric region is indeed where the SIRC model displays the richest variety of behaviors (multi-annual coexisting cycles and/or chaotic attractors). Thus, the arbitrarily selected parameter settings used for the comparison can strongly influence the results. For this reason, one can question if the approach of directly contrasting the model generated time series with prevalence data, especially in cases where the epidemiological regime is irregular in time, can be sufficient to validate a compartmental SIR-like model. It is certainly not sufficient, but we think it is necessary to verify that, at least from a qualitative viewpoint, there are temporal windows in the aperiodic simulated regime where the subtyped influenza A outbreaks are displayed as they are in some real circumstances. Fig. 5(b) shows a decadal simulation of the seasonally forced model (1) obtained by setting the parameter values as in point B of Fig. 4. We chose arbitrary initial conditions and simulate the model over a time horizon that is long enough (300 years) to avoid transient dynamics toward the strange attractor. The gray vertical strips in the same panel mark the weeks over the period 1987–1997 where some influenza A strains of subtype H3N2 were isolated in England and Wales (see data from [74]). With only one exception over a decade – the 1995–1996 epidemics is still present in the simulated time series, but as a late peak in 1996 – this model trajectory mimics impressively well the laboratory confirmed pattern.

Various quantitative epidemiological indicators evaluated for the attractor of Fig. 5(b) match also quantitatively empirical evidence from temperate countries. According to Couch [70], for example, the annual incidence varies between 0.1 and 0.21 in data and J (see Eq. (4) above) is around 0.14. The empirical attack rate is higher than incidence in data and varies in the range 0.15–0.24 (see data in [77,31,78]). We can estimate the attack rate with the SIRC model simply as $J^{\text{att}} = \frac{1}{n}\sum_{k=1}^{n} J_k$, where $J_k = \int_{k-1}^{k} \beta(\xi)[S(\xi) + \sigma C(\xi)]I(\xi)\,\mathrm{d}\xi$ represents the incidence during the kth of n epidemic seasons, i.e., the seasons where $I(t)$ has exceeded a given threshold. By choosing such a threshold in the ranges typically used in the European Influenza Surveillance Scheme (between 10^{-5} and 10^{-4}, see [79] for details), we obtain that $0.18 < J^{\text{att}} < 0.2$ for the attractor of Fig. 5(b). The average peak-to-peak return time for that attractor is approximately 1.65 – well within ranges of real epidemiological regimes, as described above – and its average peak prevalence is around 2%. Empirically, this indicator varies between 1% and 4% [80]. To analyze the robustness of these results, we evaluated the above epidemiological indicators in a sufficiently large neighborhood $\mathscr{B} = \{0.1 < \varepsilon < 0.2, 300 < \beta_0 < 600\}$ of point B in Fig. 4 and found that the predicted values are, as expected, much less sensitive to the parameter choice than the direct comparison between time series would be. More precisely, in good accordance with data, the annual incidence J and the attack rate J^{att} vary respectively between 0.12–0.15 and 0.14–0.29 in $\mathscr{B}$.

Chaos is not the only way of thinking about aperiodicity in epidemiological regimes. The irregularities at low frequency seen in incidence patterns can also be caused by stochastic transitions

between deterministic periodic attractors, as originally proposed by Schwartz [81]. In the model literature, the noise-driven switch between different regimes takes sometimes the form of a rapid change in the values attributed to the parameters (usually the transmission rate, like in [82]): any parametric change induces indeed a transient dynamics of the system toward a different attractor. More often [81,83–85] the perturbation is instead introduced into the model as a rapid change in the values of the state variables for a fixed – yet particular – parameter setting, i.e., such that multiple stable periodic outbreaks can coexist. For the traditional SIR model, Schwartz [81] has first shown that the basins of attraction of multiple stable cycles 'are intertwined in a complicated manner'. The epidemiological consequence is that, even when very low levels of stochasticity are interacting with the deterministic process, shifts between attractors will certainly occur. Although Aron [83] argued that the basins' boundaries are 'possibly fractal in nature' (see p. 66), we are unaware of any proof of this. Fig. 6 shows the basins of attraction of the three stable cycles coexisting in the SIRC model for parameter settings as in point C of Fig. 4 and makes evident that the basins can indeed be fractal sets. In fact, by zooming into the boundaries of those intermixed sets of initial conditions (see Fig. 6(b) and (c)) self-similarity clearly emerges. Epidemiologically, this implies that predictability can be problematic in such cases. If the basins of attraction are fractal sets, indeed, unavoidable uncertainty on initial conditions cannot only cause quantitative errors on the exact timing and/or amplitude of the predicted outbreaks, but also can alter our prediction of the qualitative behavior of the epidemiological regime (e.g., annual vs. biennial recurrent disease). Consequently, if the dynamics can be unpredictable even under the most favorable – yet unrealistic – hypothesis of a purely deterministic epidemiological process, it is very critical to forecast what would happen in more plausible, noisy situations.

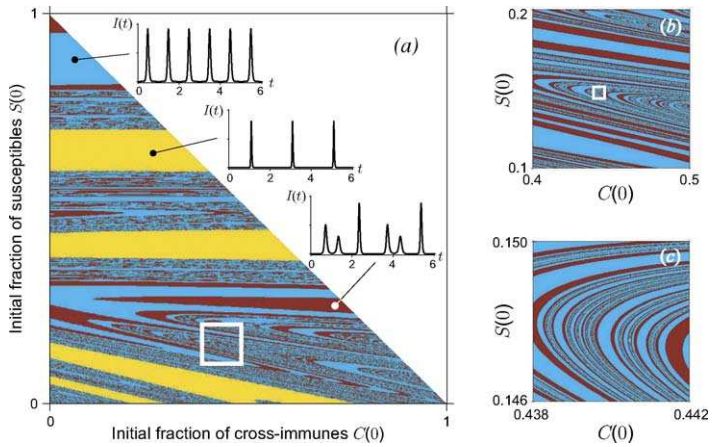

Fig. 6. Basins of attraction of the three stable cycles coexisting in the SIRC model for parameter settings as in point C of Fig. 4 and other initial states as $I(0) = 10^{-3}$ and $R(0) = 1 - I(0) - S(0) - C(0)$. Initial states in the cyan, yellow and brown sets indicate convergence to a period-one, period-two and period-three cycle, respectively (see the temporal patterns). (a) The nature of the periodic regime reached while varying the initial conditions $S(0)$ and $C(0)$ has been determined by computing the Lyapunov exponents of the attractor via standard numerical algorithms [91]. (b) As before, but for initial conditions in the 10^2 times smaller white square of (a). (c) As before, but zooming into the 25^2 times smaller white square of (b). (For interpretation of color in this figure, the reader is referred to the web version of this article.)

5. Discussion

In this article we have proposed an improvement over the classical SIR approach to study diseases where hosts can exhibit partial immunity with respect to an evolving pathogen, typically a virus. When the evolutionary process occurs on a timescale that is comparable with the ecology of the disease, as for influenza [11], mathematical methods based on singular perturbation analysis are useless and it is necessary to incorporate the viral transformations directly into the epidemiological model. The strategy adopted here has been to partition the host population into four compartments, as seen from the perspective of the currently circulating dominant strain of the virus. This unusual assumption let us drastically reduce the number of state variables required for building the non-linear epidemiological model. With the SIRC minimal model it is then easy to discuss how the different epidemiological parameters influence the recurrence of outbreaks, both in terms of frequency and intensity.

We have already investigated above how the seasonal fluctuations of the contact rate shape the epidemiological regime. Other relevant considerations can be made, for example, regarding the role of cross-immunity. As shown in Fig. 7, reducing the reinfection probability σ, i.e., increasing cross-immunity $(1-\sigma)$ and boosting $(1-\sigma)\beta$, has the effect of enlarging the regions in the parameter space (ε, β_0) where the SIRC model displays complex dynamics (see also Fig. 3(a) as a reference). Since in the limit of $\sigma \to 1$, that is for an SIRS model, the same regions are much smaller, we can conclude that cross-immunity and boosting are crucial to inducing complicated regimes when parameter values are in plausible ranges for influenza. Thus, our findings reinforce those already obtained with alternative models [86,73,13,87].

Once a core model is analyzed and the results obtained are promising, it is hard to resist the temptation of introducing variants. In order to mimic the ILI temporal patterns, it could be possible to couple more SIRC-like models to deal with competing viral subtypes. The same method can be used to understand how the virus can transmit between the Southern and the Northern hemisphere every flu season. These extensions would require at least doubling the number of state variables of the model. Even without changing the model, however, other interesting analyses

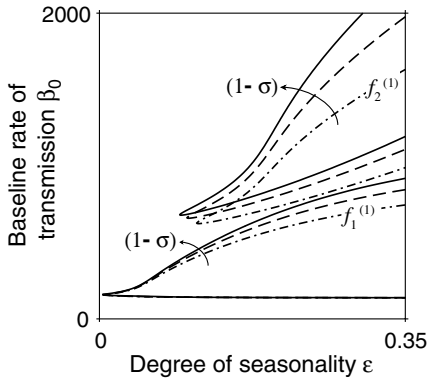

Fig. 7. The effect of increasing cross-immunity $(1-\sigma)$ on the skeleton of the parametric portrait of the SIRC model. All the curves are flip bifurcations involving period-one attractors. Solid is for $\sigma = 0.07$, dashed for $\sigma = 0.1$, dashed and dotted for $\sigma = 0.15$. Unspecified parameters as in Fig. 3.

could be performed. One natural improvement is that of implementing vaccination programs. For example, the CDC proposes to vaccinate all children aged 6–23 months against influenza (see http://www.cdc.gov/flu/). What would be the effect of such a policy on the prevalence pattern? Another relevant step would be that of understanding the effects of antiviral drugs (currently based on amantadine and rimantadine) on preventing and treating influenza A. Indeed, one of the most important advantages of minimal models is that they can be readily used as support systems for decision makers. We hope therefore that the models introduced here will be of interest not only for the preliminary results we have obtained, but also for the potential raises for extensions both on theoretical and applied consequence.

Acknowledgments

We are pleased to acknowledge Roberto Defendi for his constructive help in carrying out some of the numerical analyses. Critical discussions with Fabrizio Pregliasco, Marino Gatto, Carlo Piccardi, Juan Lin, Jonathan Dushoff and Lone Simonsen also gave us many stimuli at different stages of the work. The model has been inspired by some meetings organized at the EEB Department of Princeton University under the auspices of National Institutes of Health (grants NIH #1RO1GM607929 and #1P50GM071508-01). The Italian Ministry of University and Research (project FIRB-RBNE01CW3M) and Politecnico di Milano are also acknowledged for financial support to RC.

References

[1] A. Klimov, L. Simonsen, K. Fukuda, N. Cox, Surveillance and impact of influenza in the United States, Vaccine 17 (1999) S42.
[2] N. Cox, K. Subbarao, Global epidemiology of influenza, Ann. Rev. Med. 51 (2000) 407.
[3] L. Simonsen, M. Clarke, L. Schonberg, N. Arden, N. Cox, K. Fukuda, Pandemic versus epidemic influenza mortality: a pattern of changing age distribution, J. Infect. Diseases 178 (1998) 53.
[4] L. Simonsen, M. Clarke, G. Williamson, D. Stroup, L. Schonberger, The impact of influenza epidemics on mortality: introducing a severity index, Am. J. Public Health 87 (1997) 1944.
[5] P. Palese, J. Young, Variation of influenza A, B, and C viruses, Science 215 (1982) 1468.
[6] R. Webster, W. Bean, O. Gorman, T. Chambers, Y. Kawaoka, Evolution and ecology of influenza A viruses, Microbiol. Rev. 56 (1992) 152.
[7] R. Webster, W. Laver, G. Air, G. Schild, Molecular mechanisms of variation in influenza viruses, Nature 296 (1982) 115.
[8] H. Larson, D. Tyrrell, C. Bowker, C. Potter, G. Schild, Immunity to challenge in volunteers vaccinated with an inactivated current or earlier strain of influenza A(H3N2), J. Hyg. (Cambridge) 80 (1978) 243.
[9] J. Davies, E. Grilli, A. Smith, Influenza A: infection and reinfection, J. Hyg. (Cambridge) 92 (1984) 125.
[10] A. Levine, Viruses, W.H. Freeman & Co, New York, USA, 1992.
[11] D. Earn, J. Dushoff, S. Levin, Ecology and evolution of the flu, Trends Ecol. Evol. 17 (2002) 334.
[12] V. Andreasen, J. Lin, S. Levin, The dynamics of cocirculating influenza strains conferring partial cross-immunity, J. Math. Biol. 35 (1997) 825.
[13] J. Lin, V. Andreasen, S. Levin, Dynamics of influenza A drift: the linear three-strain model, Math. Biosci. 162 (1999) 33.
[14] J. Lin, V. Andreasen, R. Casagrandi, S. Levin, Traveling waves in a model of influenza A drift, J. Theoret. Biol. 222 (2003) 437.

[15] J. Cisternas, W. Gear, S. Levin, I.G. Kevrekidis, Equation-free modelling of evolving diseases: coarse-grained computations with individual based models, Proc. Roy. Soc.: Math. Phys. Eng. Sci. 460 (2004) 2761.
[16] J. Gog, B. Grenfell, Dynamics and selection of many-strain pathogens, Proc. Nat. Acad. Sci. USA 99 (2002) 17209.
[17] C. Pease, An evolutionary epidemiological mechanism, with applications to type A influenza, Theoret. Populat. Biol. 31 (1987) 422.
[18] P. Gill, A. Murphy, Naturally acquired immunity to influenza type A: a further prospective study, Med. J. Austr. 2 (1977) 761.
[19] C. Potter, R. Jennings, K. Nicholson, D. Tyrrel, K. Dickinson, Immunity to attenuated influenza virus WRL 105 infection induced by heterologous inactivated influenza A virus vaccines, J. Hyg. (Cambridge) 79 (1977) 321.
[20] D. Smith, A. Lapedes, J. de Jong, T. Bestebroer, G. Rimmelzwaan, A. Osterhaus, R. Fouchier, Mapping the antigenic and genetic evolution of influenza virus, Science 305 (2004) 371.
[21] N. Bailey, The Mathematical Theory of Infectious Diseases and Its Application, Griffin, London, UK, 1975.
[22] M. Gomes, L. White, G. Medley, Infection, reinfection and vaccination under suboptimal immune protection: epidemiological perspectives, J. Theoret. Biol. 228 (2004) 539.
[23] T.W. Hoskins, J.R. Davies, A.J. Smith, C.L. Miller, A. Allchin, Assessment of inactivated influenza-A vaccine after three outbreaks of influenza A at Christ's Hospital, Lancet 1 (1979) 33.
[24] A. McMichael, F. Gotch, G. Noble, P. Beare, Cytotoxic T-cell immunity to influenza, New Engl. J. Med. 309 (1983) 13.
[25] H. Hethcote, An age-structured model for pertussis transmission, Math. Biosci. 145 (1997) 89.
[26] H. Hethcote, Simulations of pertussis epidemiology in the United States: effects of adult booster vaccinations, Math. Biosci. 158 (1999) 47.
[27] W.O. Kermack, A.G. McKendrick, Contributions to the mathematical theory of epidemics: II. The problem of endemicity, Proc. Roy. Soc. Lond. A 138 (1932) 55, Reprinted in Bull. Math. Biol. 53 (1932) 57–87.
[28] H. Inaba, Kermack and McKendrick revisited: the variable susceptibility model for infectious diseases, Jpn. J. Indust. Appl. Math. 18 (2001) 273.
[29] H. Thieme, J. Yang, An endemic model with variable re-infection rate and applications to influenza, Math. Biosci. 180 (2002) 207.
[30] H. Six, W. Glezen, W. Kasel, R. Couch, C. Griffis, R. Webster, Heterogeneity of influenza viruses isolated from the Houston community during defined epidemic period, in: D. Nayak (Ed.), Genetic Variation of Viruses, Academic Press, New York, USA, 1981, p. 505.
[31] J. Fox, C. Hall, M. Cooney, H. Foy, Influenza virus infections in Seattle families, 1975–1979. I. Study design, methods and the occurrence of infections by time and age, Am. J. Epidemiol. 116 (1982) 212.
[32] W. Glezen, R. Couch, H. Six, The influenza herald wave, Am. J. Epidemiol. 116 (1982) 589.
[33] N. Ferguson, A. Galvani, R. Bush, Ecological and immunological determinants of influenza evolution, Nature 422 (2003) 428.
[34] L.J. Abu-Raddad, N.M. Ferguson, Characterizing the symmetric equilibrium of multi-strain host–pathogen systems in the presence of cross immunity, J. Math. Biol. 50 (2005) 531.
[35] R. Anderson, R. May, Population biology of infectious diseases: Part I, Nature 280 (1979) 361.
[36] R. Douglas, Influenza in man, in: E. Kilbourne (Ed.), The Influenza Viruses and Influenza, Academic Press, New York, USA, 1975, p. 395.
[37] A. Frank, L. Taber, C. Wells, J. Wells, W. Glezen, A. Parades, Patterns of shedding of myxoviruses and paramyxoviruses in children, J. Infect. Diseases 144 (1981) 433.
[38] D.A. Buonagurio, S. Nekada, J.D. Parvin, M. Krystal, P. Palese, W.M. Fitch, Evolution of human influenza a viruses over 50 years: rapid, uniform rate of change in NS gene, Science 232 (1986) 980.
[39] J.B. Plotkin, J. Dushoff, S.A. Levin, Hemagglutinin sequence clusters and the antigenic evolution of influenza A virus, Proc. Nat. Acad. Sci. USA 99 (2002) 6263.
[40] A.J. Hay, V. Gregory, A.R. Douglas, Y.P. Lin, The evolution of human influenza viruses, Proc. Roy. Soc. Lond. B 356 (2001) 1861.
[41] D.J. Smith, S. Forrest, D.H. Ackley, A.S. Perels on, Variable efficacy of repeated annual influenza vaccination, Proc. Nat. Acad. Sci. USA 96 (1999) 14001.
[42] N. Cox, C.A. Bender, The molecular epidemiology of influenza viruses, Sem. Virol. 6 (1995) 359.

[43] D.G. Luenberger, Introduction to Dynamic Systems: Theory Models and Applications, John Wiley and Sons, New York, USA, 1979.
[44] W. Kermack, A. McKendrick, A contribution to the mathematical theory of epidemics, Proc. Roy. Soc. Lond. A 115 (1927) 700.
[45] H. Hethcote, Qualitative analyses of communicable disease models, Math. Biosci. 28 (1976) 335.
[46] R. Anderson, R. May, Infectious Diseases in Humans: Dynamics and Control, Oxford Science Publication, Oxford, UK, 1991.
[47] R.M. May, R.M. Anderson, Epidemiology and genetics in the coevolution of parasites and hosts, Proc. Roy. Soc. Lond. B 219 (1983) 281.
[48] M. van Baalen, M.W. Sabelis, The dynamics of multiple infection and the evolution of virulence, Am. Natural. 146 (1995) 881.
[49] A.P. Galvani, Epidemiology meets evolutionary ecology, Trends Ecol. Evol. 18 (2003) 132.
[50] C. Spicer, C. Lawrence, Epidemic influenza in greater London, J. Hyg. (Cambridge) 93 (1984) 105.
[51] A. Frank, L. Taber, C. Porter, Influenza B virus reinfection, Am. J. Epidemiol. 125 (1987) 576.
[52] R. Hope-Simpson, D. Golubev, A new concept of the epidemic process of influenza A virus, Epidemiol. Infect. 99 (1987) 5.
[53] S.F. Dowell, Seasonal variation in host susceptibility and cycles of certain infectious diseases, Emerg. Infect. Diseases 7 (2001) 369.
[54] J. Nguyen-Van-Tam, C. Brockway, J. Pearson, A. Hayward, D. Fleming, Excess hospital admissions for pneumonia and influenza in persons $\geqslant$65 years associated with influenza epidemics in three english dealt districts: 1987–1989, Epidemiol. Infect. 126 (2001) 71.
[55] W. London, J. Yorke, Recurrent outbreaks of measles, chickenpox and mumps. I. Seasonal variation in contact rate, Am. J. Epidemiol. 98 (1973) 458.
[56] J. Yorke, W. London, Recurrent outbreaks of measles, chicken pox and mumps. II. Systematic differences in contact rates and stochastic effects, Am. J. Epidemiol. 98 (1973) 469.
[57] K. Dietz, The incidence of infectious diseases under the influence of seasonal fluctuations, Lect. Notes Biomath. 11 (1976) 1.
[58] J.R. Gog, G.F. Rimmelzwaan, A.D.M.E. Osterhaus, B.T. Grenfell, Population dynamics of rapid fixation in cytotoxic T lymphocyte escape mutants of influenza A, Proc. Nat. Acad. Sci. USA 100 (2003) 11143.
[59] J. Guckenheimer, P. Holmes, Nonlinear Oscillations, Dynamical Systems and Bifurcations of Vector Fields, Springer, New York, USA, 1983.
[60] A.I. Khibnik, Y.A. Kuznetsov, V.V. Levitin, E.V. Nikolaev, Continuation techniques and interactive software for bifurcation analysis of ODEs and iterated maps, Physica D 62 (1993) 360.
[61] E.J. Doedel, J.P. Kernévez, AUTO: software for continuation and bifurcation problems in ordinary differential equations, Applied Mathematics Report, California Institute of Technology, Reading, MA, USA, 1986.
[62] Y. Kuznetsov, Elements of Applied Bifurcation Theory, Springer, New York, USA, 1995.
[63] J.L. Aaron, I.B. Schwartz, Seasonality and period-doubling bifurcations in an epidemic model, J. Theoret. Biol. 110 (1984) 665.
[64] Y. Kuznetsov, C. Piccardi, Bifurcation analysis of periodic SEIR and SIR epidemic model, J. Math. Biol. 32 (1994) 109.
[65] L. Simonsen, The global impact of influenza on morbidity and mortality, Vaccine 17 (1999) S3.
[66] A. Hampson, Epidemiological data on influenza in Asian countries, Vaccine 17 (1999) S19.
[67] L.P.-C. Shek, B.-W. Lee, Epidemiology and seasonality of respiratory tract virus infections in the tropics, Paediatr. Resp. Rev. 4 (2003) 105.
[68] F. Chew, S. Doraisingham, A. Ling, G. Kumarasinghe, B. Lee, Seasonal trends of viral respiratory tract infections in the tropics, Epidemiol. Infect. 121 (1998) 121.
[69] L. Simonsen, Influenza-related morbidity and mortality among children in developed and developing countries, Int. Cong. Ser. 1219 (2001) 13.
[70] R. Couch, Advances in influenza virus vaccine research, Ann. NY Acad. Sci. 685 (1993) 803.
[71] K.A. Fitzner, S.M. McGhee, A.J. Hedley, K.F. Shortridge, Influenza surveillance in Hong Kong: results of a trial Physician Sentinel Programme, Hong Kong Med. J. 5 (1999) 87.

[72] J. Dushoff, J.B. Plotkin, S. Levin, D. Earn, Dynamical resonance can account for seasonality of influenza epidemics, Proc. Nat. Acad. Sci. USA 101 (2004) 16915.
[73] S. Gupta, N. Ferguson, R. Anderson, Chaos persistence and evolution of strain structure in antigenically diverse infectious agents, Science 280 (1998) 912.
[74] D. Fleming, M. Zambon, A. Bartelds, Population estimates of persons presenting to general practitioners with influenza-like illness, 1987–1996: a study of the demography of influenza-like illness in sentinel practice networks in England and Wales, and in The Netherlands, Epidemiol. Infect. 124 (2000) 245.
[75] S. Rinaldi, R. Casagrandi, A. Gragnani, Reduced order models for the prediction of extreme episodes, Chaos Solitons Fract. 12 (2001) 313.
[76] J. Watson, Surveillance of influenza, in: K. Nicholson, R. Webster, A. Hay (Eds.), Textbook of Influenza, Blackwell Science Ltd., Oxford, UK, 1998, p. 207.
[77] W. Glezen, R. Couch, Interpandemic influenza in the Houston area, 1974–76, New Engl. J. Med. 298 (1978) 587.
[78] J. Nguyen-Van-Tam, Epidemiology of influenza, in: K. Nicholson, R. Webster, A. Hay (Eds.), Textbook of Influenza, Blackwell Science Ltd., Oxford, UK, 1998, p. 181.
[79] J. Aguilera, J. Paget, J. Manuguerra, Survey of influenza surveillance systems in Europe, Final report, EISS, EUROGROG (2001), URL: <http://www.eiss.org/documents/inventory_survey.pdf>.
[80] L. Toubiana, A. Flahault, A space-time criterion for early detection of epidemics of influenza-like-illness, Euro. J. Epidemiol. 14 (1998) 465.
[81] I. Schwartz, Multiple stable recurrent outbreaks and predictability in seasonally forced nonlinear epidemic models, J. Math. Biol. 21 (1985) 347.
[82] M. Keeling, P. Rohani, B. Grenfell, Seasonally forced disease dynamics explored as switching between attractors, Physica D 148 (2001) 317.
[83] J. Aron, Multiple attractors in the response to a vaccination program, Theoret. Populat. Biol. 38 (1990) 58.
[84] D.J.D. Earn, P. Rohani, B.M. Bolker, B.T. Grenfell, A simple model for complex dynamical transitions in epidemics, Science 287 (2000) 667.
[85] P. Rohani, M.J. Keeling, B.T. Grenfell, The interplay between determinism and stochasticity in childhood diseases, Amer. Natural. 159 (2002) 469.
[86] C. Castillo-Chavez, H.W. Hethcote, V. Andreasen, S.A. Levin, W.M. Liu, Epidemiological models with age-structure, proportionate mixing, and cross-immunity, J. Math. Biol. 27 (1989) 233.
[87] M. Kamo, A. Sasaki, The effect of cross-immunity and seasonal forcing in a multi-strain epidemic model, Physica D 165 (2002) 228.
[88] J.D. Murray, Mathematical Biology, Springer, Berlin, Germany, 1989.
[89] V. Andreasen, Dynamics of annual infleunza A epidemics with immuno-selection, J. Math. Biol. 46 (2003) 504.
[90] M. Boni, J. Gog, V. Andreasen, F. Christiansen, Influenza drift and epidemic size: the race between generating and escaping immunity, Theoret. Populat. Biol. 65 (2004) 179.
[91] K. Ramasubramanian, M. Sriram, A comparative study of computation of Lyapunov spectra with different algorithms, Physica D 139 (2000) 72.